Overview of Circuit Topologies for Inductive Pulsed Power Supplies

Xinjie Yu, *Member, IEEE* and Xukun Liu, *Student Member, IEEE*

(Invited)

***Abstract*—The pulsed power supply (PPS) is one important component in the electromagnetic launch system. The inductive PPSs have attracted researchers' attentions with the major advantages of high energy storage density (over the capacitive PPSs) as well as simple structure and easy control (over the rotating mechanical PPSs). As for the inductive PPSs, the circuit topology of the basic module will directly determine the comprehensive performance of the whole system. From the perspectives of working principles, strengths, weaknesses, and comprehensive performance, this paper presents a historical and technical review of the major circuit topologies for the inductive PPSs.**

***Index Terms*—Circuit topology, electromagnetic railgun, inductive energy storage, inductive pulsed power supply, meat grinder, XRAM.**

I. Introduction

With the advantages of high muzzle velocity and low money cost, the electromagnetic railguns have become a research focus in the field of military equipment [1]-[4]. The whole system is generally composed of the pulsed power supplies (PPSs) and the railgun load. The function of the PPSs is to output millisecond-, megampere, and gigawatt-level current pulse to the railgun load. And the function of the railgun load is to accelerate the projectile with the energy from the PPSs.

According to different energy storage forms, PPSs can be classified into three major kinds, namely, capacitive, inductive, and rotating mechanical [5]-[6]. For preciseness, the inductive PPSs in this paper only refer to the ones that can use DC sources as the feeding power supplies. The pulse forming/shaping inductors in the capacitive and rotating mechanical PPSs are excluded from discussion, because they are not the major energy storage components and cannot work independently.

Compared with the capacitive PPSs, the inductive PPSs generally possess one-order higher energy storage density. Compared with the rotating mechanical PPSs, the inductive PPSs are simpler in structure and easier to control. Good application prospects in mobile systems make the inductive PPSs an attractive option for the electromagnetic railguns [7]-[8].

Because the circuit topology of the basic module will determine the comprehensive performance of the whole system, circuit topology study has been one important focus in the field of the inductive PPSs. This paper presents a historical and technical review of the major circuit topologies for the inductive PPSs. As far as these circuit topologies in concern, the working principles, strengths, and weaknesses are analyzed in Section II, and the comprehensive performance is compared in Section III.

II. Circuit Topologies

The major circuit topologies for the inductive PPSs include the XRAM (backward spelling of the high voltage generation device "MARX"), the XRAM with classic ICCOS (Inverse Current COmmutation with Semiconductor devices), the XRAM with modified ICCOS, the meat grinder, the STRETCH (Slow TRansfer of Energy Through Capacitive Hybrid) meat grinder, the STRETCH meat grinder with ICCOS, the meat grinder with SECT (SElf-charged Capacitor and Thyristors), the meat grinder with CPFU (Capacitive Pulse Forming Unit) [9]. Apart from the above ones, there are some other circuit topologies, such as the ringer, the non-mutual inductance PPS, and the XRAM with magnetic flux compression effect [10]-[13]. Because of practical feasibility reasons, they are not being further studies or widely applied now, thus they are excluded from discussion. A historical evolution spectrum of the major circuit topologies is shown in Fig. 1.

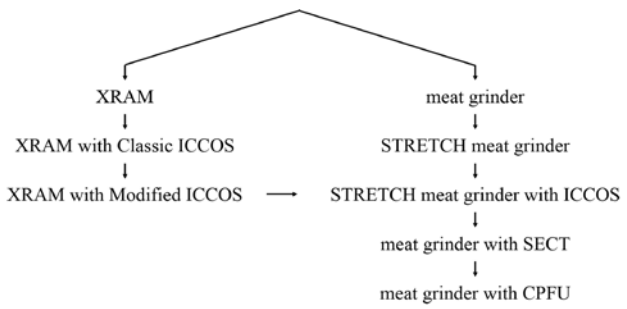

Fig. 1. Historical evolution spectrum of the circuit topologies for the inductive PPSs.

This work was supported in part by the National Natural Science Foundation of China under Grant 50877039 and in part by the Tsinghua University Initiative Scientific Research Program under Grant No. 20121087927 *(Corresponding author: Xinjie Yu)*.

The authors are with the Department of Electrical Engineering, Tsinghua University, Beijing, China and State Key Laboratory of Power System, Beijing, China (e-mail: yuxj@tsinghua.edu.cn; liuxukuncn@163.com).

A. Fundamental Circuit Topologies

A single inductor can only output the current it has been charged with. Addition and multiplication are two fundamental principles to obtain higher output currents. And the XRAM and the meat grinder correspond to these two principles, respectively.

- *XRAM*

The XRAM was proposed by Werner Koch from Marx High Voltage Institute at Brunswick Technical University in 1967 [14]-[15]. Also, the CMIS (Cuttent Multiplier by Inductive Storage) developed by the Japan Steel Works Ltd. is a XRAM in essence [16]. The schematic of the XRAM is shown in Fig. 2, where U_S is the feeding power supply, L_1, L_2, …, L_n are the energy storage inductors, R_L and L_L represent the load, S_1, S_2, …, S_n are the main switches, T_L is the load thyristor, and D_{11}, D_{12}, D_{21}, D_{22}, …, D_{n1}, D_{n2} are diodes.

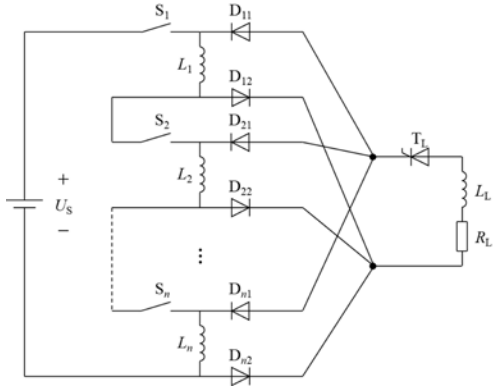

Fig. 2. Schematic of the XRAM.

The working principle of the XRAM is not complicated. First, with S_1, S_2, …, S_n closed and T_L not triggered yet, L_1, L_2, …, L_n are charged in series by U_S. Then, with S_1, S_2, …, S_n opened and T_L triggered, L_1, L_2, …, L_n discharge in parallel to the load. Because the load current is the sum of all inductor currents, the XRAM realize an addition operation of the charging current. The descriptive simulation waveforms of a four-stage XRAM are shown in Fig. 3.

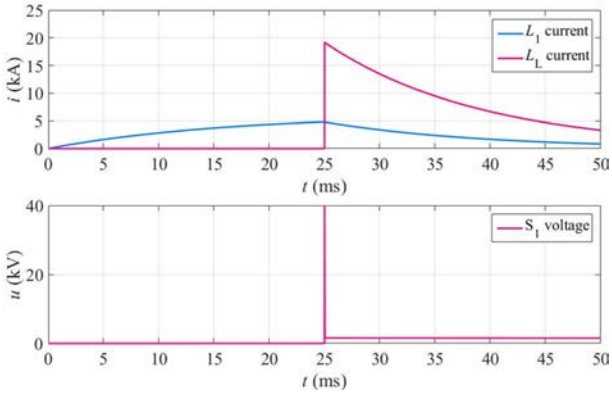

Fig. 3. Descriptive simulation waveforms of a four-stage XRAM. Parameters for simulation are listed in Table A.I in the Appendix.

One strength of the XRAM is easy modularization. Once the first stage (namely S_1, L_1, D_{11}, D_{12}) is designed and constructed, the whole system is a simple extension of multiple stages. One weakness is large main switch voltage stress. At the circuit switching moment, i.e., when t is 25 ms in Fig. 3, the load current rises in an instant. As a result, due to the load inductance, an unacceptably high commutation voltage will be generated across S_1, S_2, …, S_n. Another weakness is too many switches, which will increase module volume and decrease energy storage density.

- *Meat Grinder*

The meat grinder is proposed by Oved Zucker and et al from the Energy Compression Research Corporation in 1980 [17]-[18]. Its schematic is shown in Fig. 4, in which U_S is the feeding power supply, L_1 and L_2 are the tightly-coupled energy storage inductors, R_L and L_L represent the load, S is the main switch, and D_1 is the load diode.

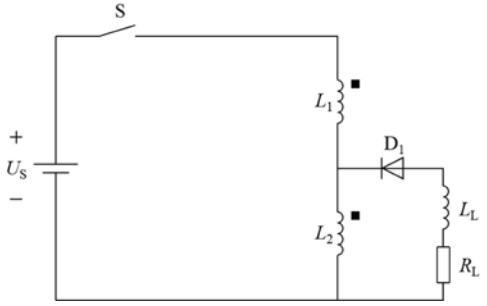

Fig. 4. Schematic of the meat grinder.

The working principle of the meat grinder is totally different from that of the XRAM. First, with S closed, L_1 and L_2 are charged in series by U_S. Then, with S opened, the current of L_1 is instantly decreased to zero, and the energy stored in L_1 and the mutual inductance between L_1 and L_2 is instantly transferred to L_2, which leads to the multiplication operation of the charging current in L_2. Afterwards, L_2 supplies the load. This current multiplication principle is also called as the magnetic flux compression principle. Because the current multiplication ratio is determined by the inductance ratio of L_1 over L_2 (see (1)), the meat grinder is a multiplication operation in essence. The descriptive simulation waveforms are shown in Fig. 5.

$$I_{\text{L-max}} = \left(1+\sqrt{\frac{L_1}{L_2}}\right) I_{\text{1-max}} \tag{1}$$

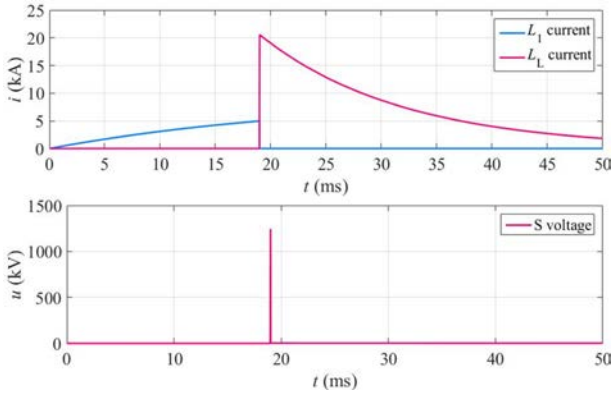

Fig. 5. Descriptive simulation waveforms of a meat grinder. Parameters for simulation are listed in Table A.II in the Appendix.

One strength of the meat grinder over the XRAM is that it is easier to achieve high current multiplication ratio, as long as L_1

is much larger than L_2. Another strength is that fewer switches are needed. One weakness is the same with that of the XRAM, namely large main switch voltage stress. In reality, L_1 and L_2 cannot be perfectly coupled. The energy in the inductor leakage flux cannot be transferred to L_2 at the circuit switching moment. Meanwhile, the commutation voltage caused by the load inductance is amplified through the coupling of L_1 and L_2, which are a set of autotransformer in essence. Both of the above two factors will result in an extremely high voltage across S.

B. Derivative Circuit Topologies of XRAM

In order to solve the main switch voltage problem and turn off higher charging current, Philipp Dedie and et al from the French-Germany Institute of Saint-Louis applied the ICCOS technique to the XRAM in 2008 [19]-[22].

- *XRAM with Classic ICCOS*

The schematic of the single-stage XRAM with classic ICCOS is shown in Fig. 6. On the basis of the schematic of the XRAM, a counter-current branch composing of a counter-current capacitor C_1 and a thyristor T_{C1} is introduced across the main switch T_1.

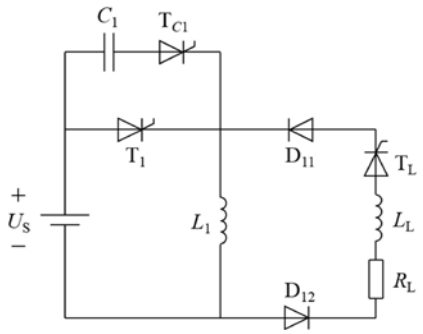

Fig. 6. Schematic of the single-stage XRAM with classic ICCOS.

The working principle of the XRAM with classic ICCOS is similar with that of XRAM. The difference is the circuit switching process. In the XRAM, the main switch S_1, S_2, …, S_n is directly opened. In the XRAM with classic ICCOS, by triggering T_{C1}, the precharged C_1 generates a counter-current pulse and forces the current of T_1 to drop below zero. Then, the current of C_1 is rapidly decreased to zero, and the load current is rapidly (but not instantly) increased to the current of L_1. Afterwards, L_1 will supply the load. The descriptive simulation waveforms of a four-stages XRAM with classic ICCOS are shown in Fig. 7.

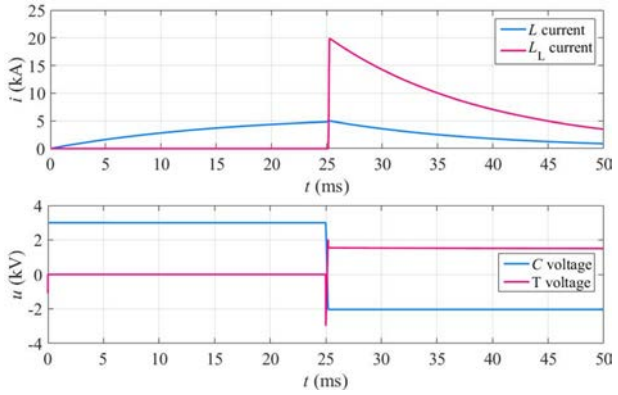

Fig. 7. Descriptive simulation waveforms of a four-stage XRAM with classic ICCOS. Parameters for simulation are listed in Table A.I in the Appendix.

One strength of the XRAM with classic ICCOS over the XRAM is that the main switch voltage stress is dramatically alleviated. Another strength is that the ICCOS technique possesses the capability of interrupting tens of kilo-ampere current, which is much stronger than that of the fully-controlled semiconductor switches. One weakness is that the additional C_1 and T_{C1} will increase module volume and decrease energy storage density.

- *XRAM with Modified ICCOS*

The schematic of the single-stage XRAM with modified ICCOS is shown in Fig. 8. On the basis of the schematic of the XRAM with Classic ICCOS, the placement of the counter-current branch is modified, not across T_1 but across D_{11}.

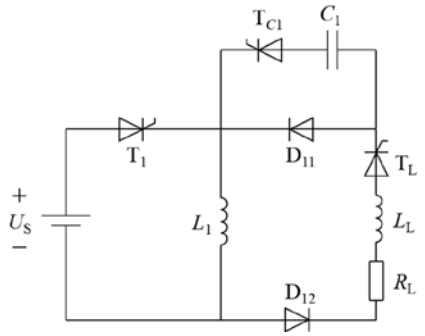

Fig. 8. Schematic of the single-stage XRAM with modified ICCOS.

The working principle of the XRAM with modified ICCOS is similar with that of the XRAM with classic ICCOS. The difference is the discharge path of C_1. In the XRAM with classic ICCOS, C_1 discharges through the path "$C_1 \rightarrow T_{C1} \rightarrow T_1 \rightarrow C_1$", so the load current rises after the counter-current pulse. But in the XRAM with modified ICCOS, C discharges through the path "$C_1 \rightarrow T_{C1} \rightarrow T_1 \rightarrow U_S \rightarrow D_{12} \rightarrow R_L \rightarrow L_L \rightarrow T_L \rightarrow C_1$", so the load current rises with the generation of the counter-current pulse. The descriptive simulation waveforms of a four-stages XRAM with modified ICCOS are shown in Fig. 9.

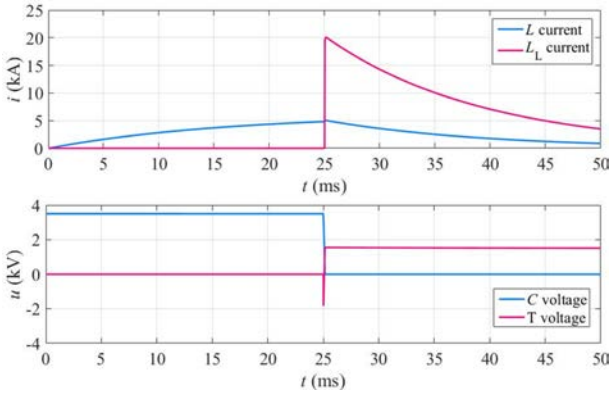

Fig. 9. Descriptive simulation waveforms of a four-stage XRAM with modified ICCOS. Parameters for simulation are listed in Table A.I in the Appendix.

One strength of the XRAM with modified ICCOS over the XRAM with classic ICCOS is lower main switch voltage stress.

The rapid rising process of the load current coincides with the generation process of the counter-current pulse. At this time, T_1 is not turned off yet. Thus, the commutation voltage caused by the load inductance has smaller influence on T_1. Another strength is that the final voltage of C_1 is zero rather than the minus of the voltage of U_S, thus all the precharged energy of C_1 can be feed into L_1 and the load. One weakness is that higher pre-charged voltage of C_1 is needed. The reason is that U_S and the load are included in the discharge path of C_1. With U_S included, the generation of the counter-current pulse has to overcome an additional voltage source; with the load included, the total inductance in the discharge path is considerably higher, therefore, higher precharged voltage is needed to achieve the same magnitude counter-current pulse.

C. Derivative Circuit Topologies of Meat Grinder

In order to improve the performance of the meat grinder, a series of circuit topologies have been successively proposed.

- *STRETCH Meat Grinder*

The STRETCH meat grinder was proposed by Alex Sitzman and et al from the University of Texas at Austin in 2005 [23]-[25]. Its schematic is shown in Fig. 10. On the basis of the schematic of the meat grinder, an energy transfer capacitor C_1, a diode D_2, and a thyristor T_3 is added.

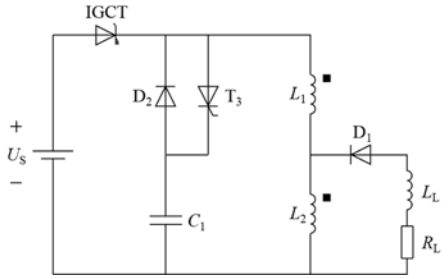

Fig. 10. Schematic of the STRETCH meat grinder.

The working process of the STRETCH meat grinder is extended based on that of the meat grinder. The magnetic flux compression principle for current multiplication is inherited. Furthermore, C_1 performs the function of absorbing the energy in the inductor leakage flux and clamping the voltage of the main switch IGCT (Integrated Gate Commutated Thyristor). Later when L_2 supplies the load, by triggering T_3, the absorbed energy in C_1 can be released to the load to generate another current peak. The descriptive simulation waveforms are shown in Fig. 11.

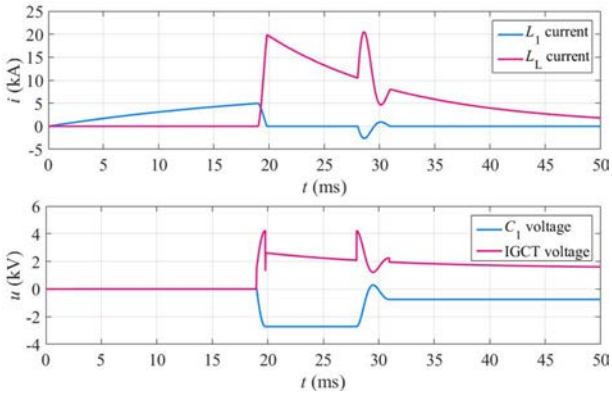

Fig. 11. Descriptive simulation waveforms of a STRETCH meat grinder. Parameters for simulation are listed in Table A.II in the Appendix.

One strength of the STRETCH meat grinder over the meat grinder is that the main switch voltage stress is decreased to acceptable level, which is resulted from the introduction of C_1. Another strength is that the energy in the inductor leakage flux can be reused to generate another load current peak. One weakness is that the additional C_1, D_2, and T_3 will increase module volume and decrease energy storage density.

- *STRETCH Meat Grinder with ICCOS*

The STRETCH meat grinder with ICCOS was proposed by Xinjie Yu and et al from Tsinghua University in 2012 [26]-[27]. Its schematic is shown in Fig. 12. On the basis of the schematic of the STRETCH meat grinder, a thyristor T_1 replaces the IGCT as the main switch. And a counter-current branch composing of a counter-current capacitor C_2 and a thyristor T_2 is introduced across L_1 and D_1.

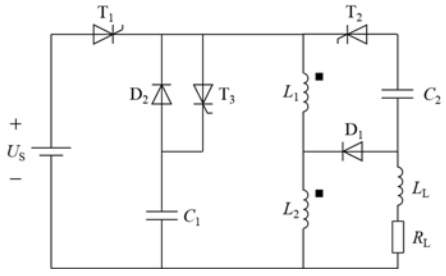

Fig. 12. Schematic of the STRETCH meat grinder with ICCOS.

The working process the STRECTH meat grinder with ICCOS is a combination of those of the STRETCH meat grinder and the XRAM with modified ICCOS. To be specific, when T_1 should be turned off, T_2 is triggered, a counter-current pulse will be generated by the precharged C_2 through the path "$C_2 \rightarrow T_2 \rightarrow T_1 \rightarrow U_S \rightarrow R_L \rightarrow L_L \rightarrow C_2$" and then turn off T_1. The subsequent working process after the turn-off of T_1 is the same as that of the STRETCH meat grinder. The descriptive simulation waveforms are shown in Fig. 13.

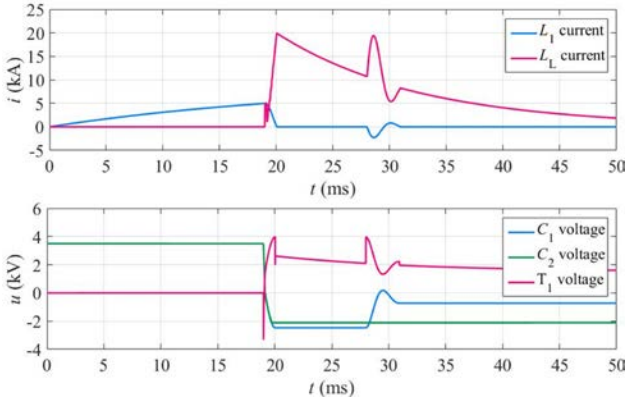

Fig. 13. Descriptive simulation waveforms of a STRETCH meat grinder with ICCOS. Parameters for simulation are listed in Table A.II in the Appendix.

One strength of the STRETCH meat grinder with ICCOS over the STRETCH meat grinder is that the current interrupting capability is greatly enhanced due to the introduction of the ICCOS technique. Another strength is that the vulnerable and

expensive IGCTs are no longer needed. One weakness is that the additional C_2 and T_2 will increase module volume and decrease energy storage density.

- *Meat Grinder with SECT*

The meat grinder with SECT was proposed by Xinjie Yu and et al in 2017 [28]. Its schematic is shown in Fig. 14. On the basis of the schematic of the STRETCH meat grinder with ICCOS, the counter-current branch is removed, and a thyristor T_2 replaces the diode D_2.

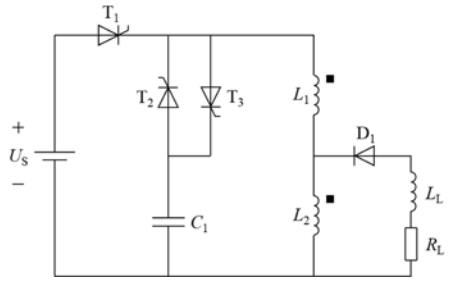

Fig. 14. Schematic of the meat grinder with SECT.

The working process the meat grinder with SECT is similar with that of the STRECTH meat grinder with ICCOS. The difference is the turn-off process of T_1. In the STRETCH meat grinder with ICCOS, T_1 is turned off by the counter-current pulse generated by the precharged C_2. But in the meat grinder with SECT, T_1 is turned off by the counter current pulse generated by the precharged C_1. In essence, the core improvement of the meat grinder with SECT is to merge C_1 and C_2 in the STRECTH meat grinder with ICCOS. The descriptive simulation waveforms are shown in Fig. 15.

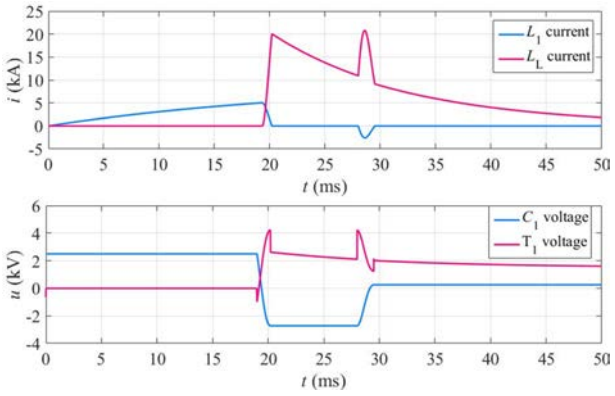

Fig. 15. Descriptive simulation waveforms of a meat grinder with SECT. Parameters for simulation are listed in Table A.II in the Appendix.

One strength of the meat grinder with SECT over the STRETCH meat grinder with ICCOS is that the removal of the ICCOS branch decreases module volume and increases energy storage density. Another strength is that it has potential to achieve the self-recovery of the precharged voltage of C_1, as long as the parameters are elaborately selected [28]. However, it should be admitted, it is not easy to achieve voltage self-recovery in practice.

- *Meat Grinder with CPFU*

The meat grinder with CPFU was proposed by Xukun Liu and Xinjie Yu in 2017 [30]. Its schematic is shown in Fig. 16. On the basis of the schematic of the meat grinder with SECT, the placement of the thyristor T_3 is modified, and a small inductor L_C is introduced.

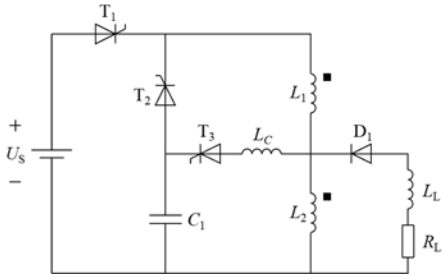

Fig. 16. Schematic of the meat grinder with CPFU.

The working process the meat grinder with CPFU is similar with that of the meat grinder with SECT. The difference is the discharge path of the C_1. In the meat grinder with SECT, C_1 releases the absorbed inductor leakage flux energy to the load through the path "$C_1 \rightarrow R_L \rightarrow L_L \rightarrow D_1 \rightarrow L_1 \rightarrow T_3 \rightarrow C_1$". But in the meat grinder with CPFU, C_1 releases the energy directly to the load through the path "$C_1 \rightarrow R_L \rightarrow L_L \rightarrow D_1 \rightarrow L_C \rightarrow T_3 \rightarrow C_1$". The descriptive simulation waveforms are shown in Fig. 17.

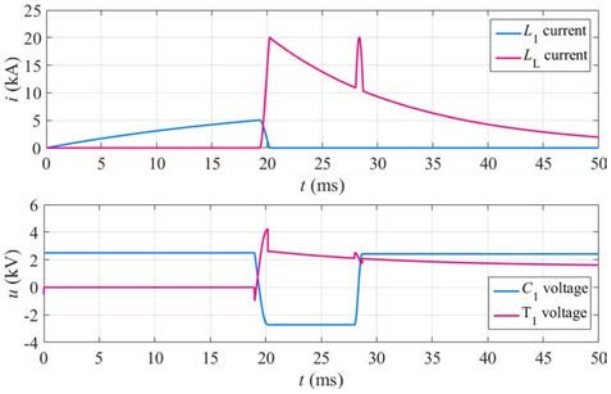

Fig. 17. Descriptive simulation waveforms of a meat grinder with CPFU. Parameters for simulation are listed in Table A.II in the Appendix.

One strength of the meat grinder with CPFU over the meat grinder with SECT is that the self-recovery rate of the precharged voltage of C_1 is much higher, which can easily exceed 100% in reality. The specific reason is that the discharge paths of C_1 and the equivalent loop resistances are different [30]. 100% self-recovery rate signifies that C_1 needs no recharges after the first operation, which is beneficial in repetitive operations. One weakness is that the additional L_C will increase module volume and decrease energy storage density. However, this problem is not that serious, because multiple modules can share one set of T_3 and L_C.

III. Performance Comparison

The comprehensive performance of 50-kJ modules based on the above circuit topologies is quantitatively compared in this Section. The estimation of the performance indices is based on theoretical calculations, numerical simulations, and engineering experiences [31]-[33]. The requirements for

module design are listed in Table I. The parameters for performance estimating are listed in Tables A.I and A.II. The comparison results of the performance indices are summarized in Tables II-III.

In general, the meat grinder series circuit topologies have smaller module volume, higher energy storage density, and lower money cost than the XRAM series circuit topologies. And the meat grinder with CPFU is the attractive option with best performance.

TABLE I
REQUIREMENTS FOR MODULE DESIGN

Categories	Parameters	Requirements
feeding power source	voltage	1500 V
energy storage inductors	total inductance	≈ 4 mH
	charging current	≈ 5 kA
	total energy	= 50 kJ
load	inductance	= 2 μH
	resistance	= 2.5 mΩ
	peak current	> 20 kA
	pulse width (> 5 kA)	> 10 ms

TABLE II
COMPARISON OF MAJOR PERFORMANCE INDICES

Circuit topologies	XRAM with classic ICCOS	XRAM with modified ICCOS	STRETCH meat grinder	STRETCH meat grinder with ICCOS	Meat grinder with SECT	Meat grinder with CPFU
Main Switch voltage stress	2.98 kV	1.83 kV	2.92 kV	3.97 kV	4.22 kV	4.22 kV
Capacitor voltage self-recovery	-67.9% (C_1)	0% (C_1)	--	-60.3% (C_2)	10.2% (C_1)	96.7% (C_1)
Module total energy*	50 + 0.9 kJ	50 + 1.2 kJ	50 + 0 kJ	50 + 2.0 kJ	50 + 2.7 kJ	50 + 2.7 kJ
Module total volume	28.1 dm^3	28.5 dm^3	17.2 dm^3	16.6 dm^3	14.2 dm^3	15.2 dm^3
Module energy storage density	1.8 MJ/m^3	1.8 MJ/m^3	2.9 MJ/m^3	3.1 MJ/m^3	3.7 MJ/m^3	3.5 MJ/m^3
Module total money cost	$12,000	$12,100	$10,700	$7,300	$6,700	$7,200

* inductive + capacitive.

TABLE III
COMPARISON OF MODULE VOLUME PROPORTIONS AND MONEY COST PROPORTIONS OF INDUCTORS, CAPACITORS, AND SWITCHES

Circuit topologies	XRAM with classic ICCOS	XRAM with modified ICCOS	STRETCH meat grinder	STRETCH meat grinder with ICCOS	Meat grinder with SECT	Meat grinder with CPFU
Module volume proportion	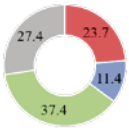	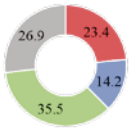	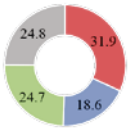	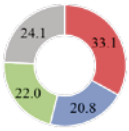	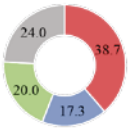	
Money cost proportion	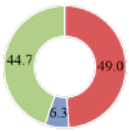	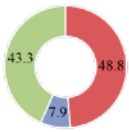	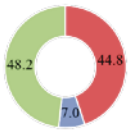	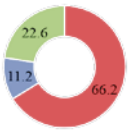	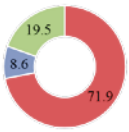	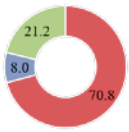

IV. CONCLUSION AND FUTURE DIRECTION

The XRAM and the meat grinder are two fundamental circuit topologies to obtain high currents. The XRAM with classic ICCOS, the XRAM with modified ICCOS, the STRETCH meat grinder, the STRETCH meat grinder with ICCOS, the meat grinder with SECT, the meat grinder with CPFU are the major derivative circuit topologies based on the XRAM and the meat grinder. This paper provides a historical and technical review of the above circuit topologies for the inductive PPSs in the electromagnetic launch system. Their working principles, strengths, and weaknesses are analyzed in details. Their comprehensive performance including main switch voltage stress, capacitor voltage self-recovery rate, module total volume, module energy storage density, and module total money cost, are compared.

In the future, in order to solve the energy recovery problem, namely to capture and reuse the energy remained in the energy storage inductors after the projectile leaves the muzzle, new circuit topologies will be developed.

ACKNOWLEDGEMENT

The authors would like to thank Dr. Harry Fair, Dr. Ian McNab, Dr. Markus Schneider, and Dr. Oliver Liebfried for the support, encouragement, and inspiration obtained in the discussion and email communication.

APPENDIX

TABLE A.I
PARAMETERS OF THE XRAM SERIES CIRCUIT TOPOLOGIES

Categories	Parameters	Circuits	Value
feeding power source U_S	voltage	I, II, III	1500 V
energy storage inductor L_1, L_2,…, L_n	stage number		4
	inductance (each stage)	I, II, III	0.9951 mH
	resistance (each stage)		60.52 mΩ
counter-current capacitor C_i	capacitance (each stage)	II, III	0.2 mF
	precharged voltage (each stage)	II	3000 V
		III	3500 V
load	inductance	I, II, III	2 μH
	resistance		2.5 mΩ
switches	turn-on time of S_i	I	0 ms
	turn-off time of S_i	I	25 ms
	triggering time of T_i	II, III	0 ms
	triggering time of T_{Ci}	II, III	25 ms
	triggering time of T_L	I, II, III	25 ms

* Circuit I: the XRAM.
Circuit II: the XRAM with classic ICCOS.
Circuit III: the XRAM with modified ICCOS.

TABLE A.II
PARAMETERS OF THE MEAT GRINDER SERIES CIRCUIT TOPOLOGIES

Categories	Parameters	Circuit	Value
feeding power source U_S	voltage	I, II, III, IV, V	1500 V
energy storage inductor L_1, L_2	primary inductance	I, II, III, IV, V	2.389 mH
	secondary inductance		0.2182 mH
	coupling coefficient		0.954
	primary resistance		146.5 mΩ
	secondary resistance		14.66 mΩ
energy transfer capacitor C_1	capacitance	IV, V	0.8 mF
	precharged voltage		2500 V
counter-current capacitor C_2	capacitance	III	0.2 mF
	precharged voltage		3500 V
load	inductance	I, II, III, IV, V	2 μH
	resistance		2.5 mΩ
switches	turn-on time of S, IGCT	I, II	0 ms
	turn-off time of S, IGCT	I, II	19 ms
	triggering time of T_1	III, IV, V	0 ms
	triggering time of T_2	III, IV, V	19 ms
	triggering time of T_3	III, IV,V	28 ms

* Circuit I: the meat grinder.
Circuit II: the STRETCH meat grinder.
Circuit III: the STRETCH meat grinder with ICCOS.
Circuit IV: the meat grinder with SECT.
Circuit V: the meat grinder with CPFU.

REFERENCE

[1] H. D. Fair, "Advances in electromagnetic launch science and technology and its application," *IEEE Trans. Magn.*, vol. 45, no. 1, pp. 225-230, Jan. 2009.

[2] I. R. McNab and F. C. Beach, "Naval railguns," *IEEE Trans. Plasma Sci.*, vol. 43, no. 1, pp. 463-468, Jan. 2007.

[3] P. Lehmann, "Overview of the electric launch activities at the French-German Institute of Saint-Louis (ISL)," *IEEE Trans. Magn.*, vol. 39, no. 1, pp. 24-28, Jan. 2003.

[4] J. Li, R. Cao, and S. Li, "The development of EML technology in China," *IEEE Trans. Plasma Sci.*, vol 41, no. 5, pp. 1029-1033, May 2013.

[5] I. R. McNab, "Pulsed power options for large EM launchers," *IEEE Trans. Plasma Sci.*, vol. 43, no 5, pp. 1352-1357, May 2015.

[6] I. R. McNab, "Large-scale pulsed power opportunities and challenges," *IEEE Trans. Plasma Sci.*, vol. 42, no 5, pp. 1118-1127, May 2014.

[7] O. Liebfried, "Review of inductive pulsed power generators for railguns," *IEEE Trans. Plasma Sci.*, vol. 45, no. 7, pp. 1108-1114, July 2017.

[8] X. Yu and X. Liu, "Review of the meat grinder circuits for railguns," *IEEE Trans. Plasma Sci.*, vol. 45, no. 7, pp. 1086-1094, July 2017.

[9] X. Liu and X. Yu, "Overview of circuit topologies for inductive pulsed power supplies," presented at 21st IEEE Int. Pulsed Power Conf., June 2017.

[10] D. Giorgi, H. Helava, K. Lindner, and et al, "The ringer: an efficient, high repetition rate circuit for electromagnetic launchers," *IEEE Trans. Magn.*, vol. 25, no. 1, pp. 203-206, Jan 1989.

[11] X. Liu, Z. Wang, and J. Li, "Circuit topology of a new inductive storage pulsed-power supply to drive railgun," *Power Syst. Technol.*, vol. 33, no. 13, pp. 80-84, Jan. 2009.

[12] X. Yu and X. Chu, "Comparisons of three inductive pulsed power supplies," *IEEE Trans. Plasma Sci.*, vol. 41, no. 5, pp. 1340-1345, May 2013.

[13] S. Ma, X. Yu, and Z. Li, "XRAM pulsed current generator with magnetic flux compression effect," *IEEE Trans. Plasma Sci.*, vol. 45, no. 7, pp. 1190-1195, July 2017.

[14] R. D. Ford and R. D. Hudson, "Novel hybrid XRAM current multiplier," *IEEE Trans. Magn.*, vol. 29, no. 1, pp. 949-953, 1993.

[15] O. Liebfried, V. Brommer, and S. Scharnholz, "Development of XRAM generators as inductive power source for very high current pulses," in *Proc. 19th IEEE Int. Pulsed Power Conf.*, Jun. 2013.

[16] Y. Aso, T. Hashimoto, T. Abe, et al, "Inductive pulsed-power supply with Marx Generator Methodology," *IEEE Trans. Magn.*, vol. 45, no. 1, pp. 237-240, 2009.

[17] O. Zucker, J. Wyatt, and K. Lindner, "The meat grinder: theoretical and practical limitations," *IEEE Trans. Magn.*, vol. MAG-20, no. 2, pp. 391-394, Mar. 1984.

[18] K. Lindner, J. Long, D. Girogi, T. Navapanich, and O. Zucker, "A meatgrinder circuit for energizing resistive and varying inductive loads (EM guns)," *IEEE Trans. Magn.*, vol. MAG-22, no. 6, pp. 1591-1596, Nov. 1986.

[19] P. Dedie, V. Brornmer, and S. Scharnholz, "ICCOS countercurrent-thyristor high-power opening switch for currents up to 28 kA," *IEEE Trans. Magn.*, vol. 45, no. 1, pp. 536-539, Jan. 2009.

[20] P. Dedie, V. Brommer, and S. Scharnholz, "Experimental realization of an eight-stage XRAM generator based on ICCOS semiconductor opening switches, fed by a magnetodynamic storage system," *IEEE Trans. Magn.*, vol. 45, no. 1, pp. 266-271, Jan. 2009.

[21] P. Dedie, V. Brommer, and S. Scharnholz, "Twenty-stage toroidal XRAM generator switched by countercurrent thyristors," *IEEE Trans. Plasma Sci.*, vol. 39, no. 1, pp. 263-267, Jan. 2011.

[22] O. Liebfried and V. Brommer, "A four-stage XRAM generator as inductive pulsed power supply for a small-caliber railgun," *IEEE Trans. Plasma Sci.*, vol. 41, no. 10, pp. 2805-2809, Oct. 2013.

[23] A. Sitzman, D. Surls, and J. A. Mallick, "STRETCH meat grinder: A novel circuit topology for reducing opening switch stress," in *Proc. 15th IEEE Int. Pulsed Power Conf.*, Jun. 2005.

[24] A. Sitzman, D. Surls, and J. Mallick, "Modification and testing of a battery-inductor repetitive pulsed power supply for a small railgun," in *Proc. 16th IEEE Int. Pulsed Power Conf.*, Jun. 2007.

[25] A. Sitzman, D. Surls, and J. A. Mallick, "Design, construction, and testing of an inductive pulsed-power supply for a small railgun," *IEEE Trans. Magn.*, vol. 43, no. 1, pp. 270-274, Jan. 2007.

[26] X. Yu and X. Chu, "STRETCH meat grinder with ICCOS," *IEEE Trans. Plasma Sci.*, vol. 41, no. 5, pp. 1346-1351, May 2013.

[27] X. Yu, S. Ma, and Z. Li, "System implementation and testing of the STRETCH meat grinder with ICCOS," *IEEE Trans. Plasma Sci.*, vol. 43, no. 5, pp. 1474-1479, May 2015.

[28] X. Yu, R. Ban, X. Liu, and et al, "The meat grinder with SECT circuit," *IEEE Trans. Plasma Sci.*, vol. 45, no. 7, pp. 1448-1452, July 2017.

[29] X. Liu, X. Yu, R. Ban, and et al, "Parameter analysis of the energy transfer capacitor in the meat grinder with SECT circuit," *IEEE Trans. Plasma Sci.*, vol. 45, no. 7, pp. 1239-1244, July 2017.

[30] X. Liu and X. Yu, "The meat grinder with CPFU: a novel circuit for inductive pulsed power supplies," *IEEE Trans. Plasma Sci.*, vol. 45, no. 9, pp. 2546-2551, Sep. 2017.

[31] X. Liu, X. Yu, and Z. Li, "Inductance calculation and energy density optimization of the tightly coupled inductors used in inductive pulsed power supplies," *IEEE Trans. Plasma Sci.*, vol. 45, no. 6, pp. 1026-1031, June 2017.
[32] X. Liu, X. Yu, R. Ban, and et al, "Analysis of the capacitive hybrid meat grinder circuits for an inductive pulsed power supply," *IEEE Trans. Plasma Sci.*, vol. 45, no. 7, pp. 1339-1346, July 2017.
[33] X. Liu, X. Yu, R. Ban, and et al, "Discussion on minimum pre-charged voltage and energy of the counter-current capacitor in ICCOS," *IEEE Trans. Plasma Sci.*, vol. 45, no. 7, pp. 1347-1352, July 2017.

Xinjie Yu (M'01) was born in Guizhou, China, in February 1973. He received B.S. and Ph.D. degrees in electrical engineering from Tsinghua University, Beijing, China, in 1996 and 2001, respectively.

He is currently an associate professor with the Department of Electrical Engineering, Tsinghua University. His current research interests include pulsed power supply, current sensors, and computational intelligence.

Xukun Liu (S'15) was born in Jiangxi, China, in May 1993. He received a B.S. degree in electrical engineering and automation from Tsinghua University, Beijing, China, in 2014.

He is currently pursuing a Ph.D. degree in electrical engineering in the Department of Electrical Engineering, Tsinghua University. His research direction is pulsed power supply.